Am J Physiol Cell Physiol 317: C1011–C1024, 2019.
First published August 21, 2019; doi:10.1152/ajpcell.00156.2019.

RESEARCH ARTICLE

The impact of skeletal muscle contraction on CD146$^+$Lin$^-$ pericytes

Svyatoslav Dvoretskiy,[1,2] Koyal Garg,[2] Michael Munroe,[1,2] Yair Pincu,[1,2] Ziad S. Mahmassani,[1,2] Charlotte Coombs,[2] Brent Blackwell,[1,2] Gabriela Garcia,[1,2] Garret Waterstradt,[1,2] Isaac Lee,[1,2] Jenny Drnevich,[3] Justin S. Rhodes,[4] and Marni D. Boppart[1,2]

[1]*Department of Kinesiology and Community Health, University of Illinois at Urbana-Champaign, Urbana, Illinois;* [2]*Beckman Institute for Advanced Science and Technology, University of Illinois at Urbana-Champaign, Urbana, Illinois;* [3]*Roy J. Carver Biotechnology Center, High Performance Biological Computing, University of Illinois at Urbana-Champaign, Urbana, Illinois; and* [4]*Department of Psychology and Neuroscience Program, University of Illinois at Urbana-Champaign, Urbana, Illinois*

Submitted 2 May 2019; accepted in final form 19 August 2019

Dvoretskiy S, Garg K, Munroe M, Pincu Y, Mahmassani ZS, Coombs C, Blackwell B, Garcia G, Waterstradt G, Lee I, Drnevich J, Rhodes JS, Boppart MD. The impact of skeletal muscle contraction on CD146$^+$Lin$^-$ pericytes. *Am J Physiol Cell Physiol* 317: C1011–C1024, 2019. First published August 21, 2019; doi:10.1152/ajpcell.00156.2019.—Unaccustomed resistance exercise can initiate skeletal muscle remodeling and adaptive mechanisms that can confer protection from damage and enhanced strength with subsequent stimulation. The myofiber may provide the primary origin for adaptation, yet multiple mononuclear cell types within the surrounding connective tissue may also contribute. The purpose of this study was to evaluate the acute response of muscle-resident interstitial cells to contraction initiated by electrical stimulation (e-stim) and subsequently determine the contribution of pericytes to remodeling as a result of training. Mice were subjected to bilateral e-stim or sham treatment. Following a single session of e-stim, NG2$^+$CD45$^-$CD31$^-$ (NG2$^+$Lin$^-$) pericyte, CD146$^+$Lin$^-$ pericyte, and PDGFRα^+ fibroadipogenic progenitor cell quantity and function were evaluated via multiplex flow cytometry and targeted quantitative PCR. Relative quantity was not significantly altered 24 h postcontraction, yet unique gene signatures were observed for each cell population at 3 h postcontraction. CD146$^+$Lin$^-$ pericytes appeared to be most responsive to contraction, and upregulation of genes related to immunomodulation and extracellular matrix remodeling was observed via RNA sequencing. Intramuscular injection of CD146$^+$Lin$^-$ pericytes did not significantly increase myofiber size yet enhanced ECM remodeling and angiogenesis in response to repeated bouts of e-stim for 4 wk. The results from this study provide the first evidence that CD146$^+$Lin$^-$ pericytes are responsive to skeletal muscle contraction and may contribute to the beneficial outcomes associated with exercise.

angiogenesis; CD146; contraction; extracellular matrix; fibroadipogenic progenitor; pericyte; remodeling; stem cells

INTRODUCTION

Mechanical strain associated with eccentric contractions during resistance exercise can cause immediate damage to the sarcolemma and disrupt myofibrillar protein structure within sarcomeres (26, 38). Skeletal muscle is highly responsive to strain and damage, initiating a molecular response to resist physiological stress with subsequent bouts of exercise (26, 28). It is well established that myogenic stem cells, satellite cells (Pax7$^+$), provide an essential role in muscle repair following acute exercise (40, 43), yet the cellular origin and full repertoire of early events that contribute to posttraining improvements in myofiber size and strength are not well defined and are the focus of intense scientific investigation (19, 20, 22, 32, 35). Elucidation of the mechanisms that drive the beneficial adaptive response to exercise is not only intriguing from a performance perspective, but may also inform the development of cell-based rehabilitation strategies to regrow muscle following a period of disuse.

Exercise initiates intracellular signaling, transcription, and translational events within the myofiber that can directly impact structure and function. The myofiber itself likely represents the primary cellular origin for skeletal muscle adaptation posttraining. However, multiple mononuclear cells resident within skeletal muscle connective tissue may also contribute to exercise-induced structural and functional gains. Satellite cells in the basal lamina, canonical connective tissue fibroblasts, immune cells, and perivascular stem/stromal cells, including pericytes and mesenchymal stem cells (MSCs), have been examined to some extent. Satellite cell elimination from skeletal muscle suggests no impact on mechanical load-induced growth in adult mice (32, 35), yet depletion appears to remove extracellular vesicle-mediated suppression of fibroblast-derived collagen synthesis, which can ultimately restrict long-term adaptation (20). Thus the coordinated responses of both satellite cells and fibroblasts (or fibroblast-like cells) may influence myofiber growth posttraining. In addition, studies suggest that macrophages influence mechanical load-induced growth (17), yet the clodronate liposome approach used to deplete macrophages in this study may also target nonmacrophage phagocytic cells. Finally, multipotent MSCs [or fibroadipogenic progenitor cells (FAPs)] and pericytes have been identified in muscle, yet their ability to promote structural and functional advantages with training remains unclear (5). Recent work from our laboratory suggests the capacity for MSCs (Sca-1$^+$CD45$^-$) to indirectly contribute to skeletal muscle growth in mice when transplantation occurs concomitant with 4 wk of eccentric exercise training (5, 50, 53). However, cell isolation based on stem cell antigen 1 (Sca-1) yields a heterogeneous population that may include both MSCs and pericytes. Further exploration is necessary to discern the rela-

Address for reprint requests and other correspondence: M. D. Boppart, Beckman Institute for Advanced Science and Technology, 405 N. Mathews Ave., MC-251, Urbana, IL 61801 (e-mail: mboppart@illinois.edu).

tive contribution of MSCs and pericytes to myofiber adaptation posttraining.

Pericytes are vascular supportive cells found in the basement membrane of microvessels within a wide variety of tissue types (2, 21). Pericytes incompletely encase and form intimate connections with several adjacent capillary endothelial cells, and this proximity allows the pericyte to provide important structural and paracrine support necessary to regulate vascular permeability, vessel diameter and blood flow, and stabilization of newly formed capillaries. Recent studies suggest that pericytes are capable of directly contributing to skeletal muscle repair following injury (4, 12, 42), yet the response of these cells to a physiological stimulus (contraction) and contribution to beneficial adaptations associated with exercise have not been explored. One of the limitations to the study of pericytes has been lack of a unique cell surface marker (2, 7). The use of different models (human, mouse) and strategies for cell isolation also makes it difficult to outline an approach for investigation. Accepted pericyte markers include neuron-glial antigen (NG2), CD146, and platelet-derived growth factor receptor-β (PDGFRβ) (2, 7, 12, 15, 39). $NG2^+$ and $CD146^+$ pericytes appear to be divergent with respect to quantity, myogenic potential, and association with different microvessels. Whereas rare $NG2^+$ pericytes uniquely localize to arterioles and display inconsistent myogenic potential (4, 11, 12, 36), CD146 pericytes are more abundant, align with multipotent MSCs, and demonstrate myogenic potential (42). Thus justification exists to explore individual and overlapping responses of $NG2^+$ and $CD146^+$ ($CD45^-CD31^-$, also lineage negative or Lin^-) pericytes to skeletal muscle contraction and subsequent involvement in promoting the beneficial effects of exercise.

The purpose of this study was to compare the response of muscle-resident interstitial cells, including two pericyte types based on differential cell surface marker expression ($NG2^+$ and $CD146^+$) and FAPs ($PDGFR\alpha^+$) to a single session of electrical stimulation (e-stim)-based contraction. Here we demonstrate that a single session did not alter the relative quantity of any cell population at 24 h following acute contraction, yet unique gene expression profiles were observed. $CD146^+Lin^-$ pericytes appeared to be most responsive to contraction, upregulating genes important for extracellular matrix (ECM) remodeling and angiogenesis. Intramuscular injection of $CD146^+Lin^-$ pericytes in combination with electrical stimulation training for 4 wk did not significantly increase myofiber size, yet increases in ECM remodeling and angiogenesis were observed. This study provides the first evidence that $CD146^+Lin^-$ pericytes are sensitive to the stimulus of skeletal muscle contraction and may contribute to the adaptive response elicited by exercise training.

MATERIALS AND METHODS

Animals

Protocols for animal use were submitted and approved by the Institutional Animal Care and Use Committee of the University of Illinois at Urbana-Champaign. Adult (15–17 wk old), C57BL/6J mice (Jackson Laboratories, Bar Harbor, ME) were used for all electrical stimulation studies. All mice were housed in a temperature-controlled animal facility maintained on a 12:12-h light-dark cycle. Mice were fed standard laboratory chow and water ad libitum.

E-Stim-Based Muscle Contraction

Acute stimulation. Male mice were subjected to a single session of bilateral electrical stimulation (e-stim) or sham treatment to serve as a control (sham) (n = 6/group, except $CD146^+Lin^-$ 24 h gene expression data, n = 4/group). All mice were anesthetized with isoflurane (2–3% isoflurane, 0.9 L/min oxygen). Both legs were shaved and aseptically prepared. Each mouse foot was placed in a miniature metal foot plate attached to the shaft of a servomotor (1300A; Aurora Scientific, Aurora, ON, Canada). The foot was placed so that it was perpendicular to the tibia. Two platinum electrodes were inserted through the skin on either side of the sciatic nerve and the nerve was activated via a stimulator and stimulus unit. The voltage was set at 25 mA (0.025 V) to induce a tetanic contraction. A range of frequencies (50–200 Hz) were then tested, and 100 Hz (0.1-ms duration) was chosen as this frequency elicited maximal peak twitch force. The plate then rotates during electrical stimulation so that the posterior (gastrocnemius, soleus) crural muscles contract eccentrically (19° of ankle plantarflexion), forcing the anterior [tibialis anterior (TA)] crural muscles to contract concentrically. After five contractions, the plate rotates in the opposite direction during electrical stimulation so that the posterior crural muscles contract concentrically (19° of ankle dorsiflexion), forcing the anterior crural muscles to contract eccentrically. Every set (5 eccentric, 5 concentric contractions) was separated by 10-s rest periods. The stimulation protocol consisted of 4 sets, or a total of 40 contractions. Force output predominantly reflects gastrocnemius muscle activity (reported in $N \cdot mm^{-1} \cdot kg\ body\ wt^{-1}$). Sedentary sham control mice were anesthetized and subjected to electrode insertion, but the muscles were not stimulated.

Extraction and Isolation of Muscle-Resident Interstitial Cells

Three and twenty-four hours after stimulation, all mice were euthanized via carbon dioxide asphyxiation. Hindlimb muscles were rapidly dissected and placed in phosphate buffered saline (PBS) + penicillin-streptomycin (P/S) solution. The gastrocnemius-soleus complex was used for isolation of cells for all experiments, except the transplantation study, in which the tibialis anterior and vastus lateralis were added to increase cell yield. Hindlimb muscles were minced with scissors and then digested in a warm bath (37°C) in a solution of dispase (LS02104; Worthington, Lakewood, NJ) and collagenase (Worthington; LS004174), both diluted at 1:70 in PBS. Every 15 min the solution was triturated using increasingly smaller serological pipettes (25 mL, 10 mL, 5 mL, and 1 mL) for a total digestion time of 1 h. After enzymatic digestion of the muscle tissue, filtered samples were incubated at 4°C with anti-mouse CD16/CD32 (1 μg per 10^6 cells; 14-0161-81; eBioscience, San Diego, CA) for 10 min to block nonspecific Fc-mediated interactions. Cells were incubated with a cocktail of monoclonal antibodies NG2-FITC (AB5320A4; EMD Millipore, Billerica, MA), CD45-APC (559864; BD Bioscience, San Jose, CA), CD31-APC (551262; BD Bioscience), CD140a-Pacific Blue (562774; BD Bioscience), and CD146-PE (134703; Biolegend, San Diego, CA), diluted in a 1% fetal bovine serum (FBS) solution. Flow cytometry analysis was performed using a BD LSRFORTESSA X-20 System. Fluorescence-activated cell sorting (FACS) was performed using a BD FACS ARIA II located at the Edward R. Madigan Laboratory (ERML, Urbana, IL). $CD146^+CD45^-CD31^-$ ($CD45^-CD31^-$ = Lineage negative, or Lin^-), $NG2^+$ Lin^-, and CD140a $(PDGFR\alpha)^+Lin^-$ cells were collected in Buffer RLT buffer (Qiagen, Germantown, MD) and frozen at −80°C for gene expression. For both flow cytometry analysis and FACS, gates were established and compensation performed using unstained, single stain, fluorescence minus one controls. For FACS, the initial mononuclear cell population (P1) is selected to remove debris, electronic noise and doublets (Fig. 1*A*), followed by selection of the lineage negative fraction (Lin^- = $CD45^-CD31^-$; P2) based on single staining, then this gate

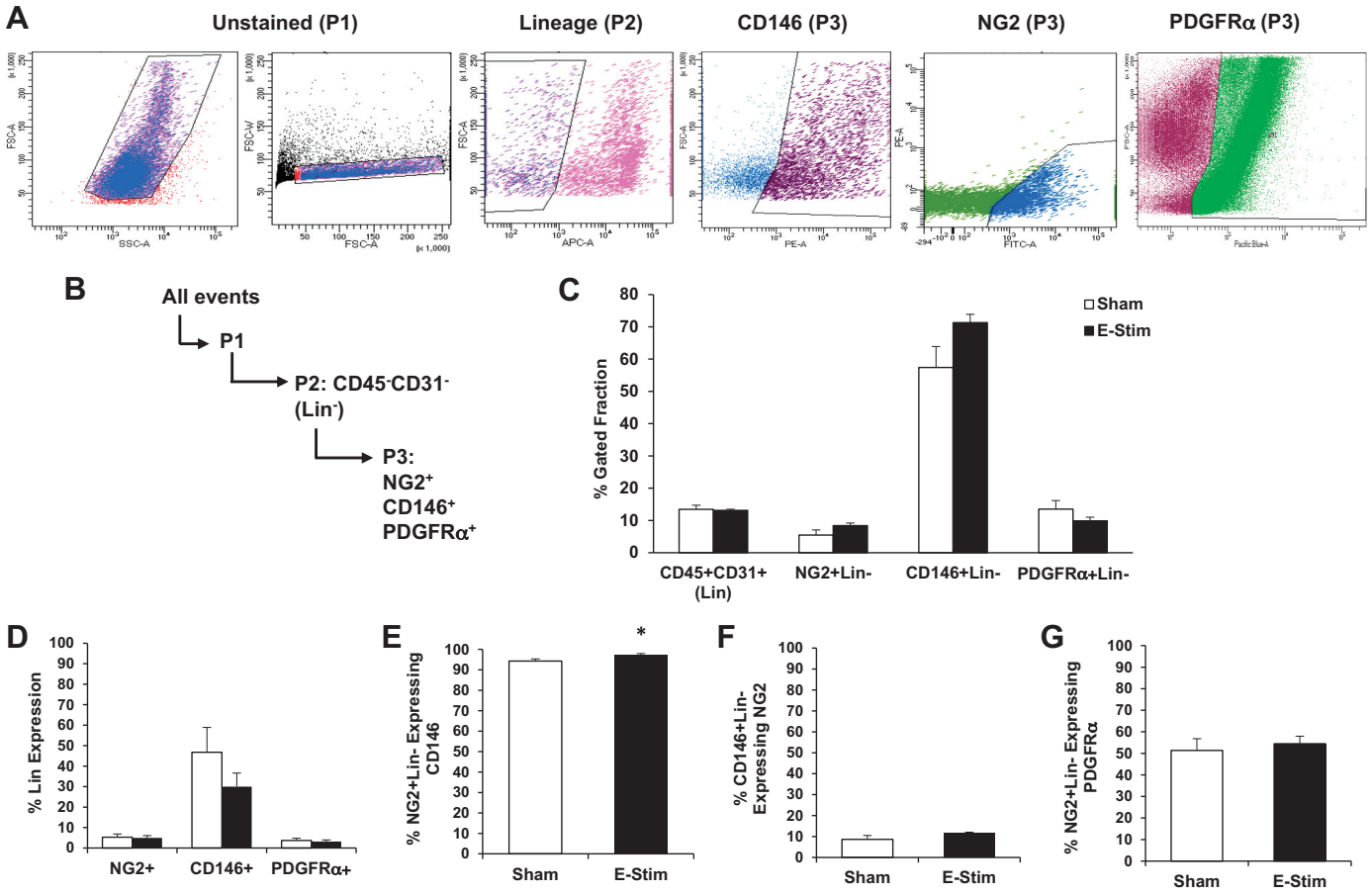

Fig. 1. Muscle-resident interstitial cell quantity is not significantly altered 24 h following acute contraction. *A*: 15- to 17-wk-old mice were subjected to an acute bout of bilateral electrical stimulation (e-stim), which induces concentric and eccentric contractions of the hindlimb muscles. Gastrocnemius-soleus complexes were harvested at 24 h post e-stim and processed for multicolor flow cytometry. NG2, neuron-glial antigen 2; PDGFRα, platelet-derived growth factor receptor-α. Gates were established and compensation performed using unstained, single stain, fluorescence minus one controls. Representative flow cytometry plots demonstrate the gating strategy for identification of $NG2^+Lin^-$, $CD146^+$ Lin^-, and $PDGFR\alpha^-Lin^+$ perivascular stem/stromal cells. *B*: gating strategy. *C*: relative cell quantity in sham and stimulated skeletal muscle. *D*: the relative percentage of cells expressing CD45 and/or CD31 (Lin). $NG2^+$ and $PDGFR\alpha^+$ cells minimally express Lin. *E*: percentage of $NG2^+Lin^-$ pericytes expressing CD146. *F*: percentage of $CD146^+Lin^-$ pericytes expressing NG2. *G*: percentage of $NG2^+Lin^-$ cells expressing PDGFRα. Values are means ± SE ($n = 4$–5). *$P < 0.05$ vs. sham.

is applied when selecting our cell type of interest after single staining for CD146, NG2, or PDGFRα (P3).

Gene Expression

RNA isolation and cDNA synthesis. RNA was extracted from cell lysates using RNeasy Micro Kit (Qiagen), following the manufacturer's instruction. Quantity and quality of isolated RNA was assessed in duplicate on a Take-3 application plate using a Synergy H1 Hybrid Multi-Mode Microplate Reader (BioTek, Winooski, VT). A starting RNA concentration of at least 10 ng was used to perform reverse transcription via the High Capacity cDNA Reverse Transcription Kit (Life Technologies, Grand Island, NY) per manufacturer's instructions.

cDNA preamplification and quantitative PCR. Preamplification of cDNA was completed using TaqMan PreAmp Master Mix Kit (Life Technologies) and inventoried Taqman primers (Applied Biosystems, Grand Island, NY). Each reaction was amplified for 14 cycles using a thermo-cycler (ABI Geneamp 9700; Life Technologies). Quantitative (q)PCR was performed using the 7900HT Fast Real-Time PCR System with Taqman Universal PCR Master Mix (Applied Biosystems). All genes were normalized to glyceraldahyde-3-phosphate dehydrogenase (*Gapdh*), which remained unchanged by the experimental procedure, and expressed relative to corresponding control condition. Gene expression data are presented using the ΔΔCt method with cycle threshold (Ct) replicate values within 0.5 Ct units. Primer information and gene expression assay ID numbers used in this study are provided in Table 1.

RNA sequencing

RNA was extracted from cell lysates using miRNeasy Mini Kit (Qiagen), following the manufacturer's instruction (RNAs ≥18 nt). Quantity and quality of isolated RNA were assessed in duplicate on a Take-3 application plate using a Synergy H1 Hybrid Multi-Mode Microplate Reader (BioTek, Winooski, VT), as well as with a bioanalyzer (2100; Agilent Technologies, Santa Clara, CA). RNA sequencing (RNA-Seq) libraries were prepared with the SMARTer Stranded Total RNAseq Kit v2 Pico Input Mammalian (Clontech, Mountain View, CA). The libraries were quantitated by qPCR and sequenced on 1 lane for 101 cycles from one end of the fragments on a HiSeq 4000 using a HiSeq 4000 sequencing kit version 1. Fastq files were generated and demultiplexed with the bcl2fastq vs2.17.1.14 conversion software (Illumina, San Diego, CA). Quality check of the raw data of the individual samples was performed by using FASTQC version 0.11.5. Average per-base read quality scores were over 30 in all samples, and no adapter sequences were found, suggesting high-quality reads. Salmon (version 0.8.2) was used to quasi-map reads to

Table 1. *Primer information and gene expression assay ID numbers*

Gene Symbol	Gene Name	Assay ID
Ang	Angiogenin	Mm00833184_s1
Bdnf	Brain-derived neurotrophic factor	Mm00833184_s1
Col1a1	Collagen type I α 1 chain	Mm00801666_g1
Col3a1	Collagen type III α1 chain	Mm01254476_m1
Col6a3	Collagen type VI α3 chain	Mm00711678_m1
Ebf1	Early B cell factor 1	Mm00432954_m1
Egf	Epidermal growth factor	Mm00438696_m1
Fgf2	Fibroblast growth factor 2	Mm01285715_m1
Fndc5	Fibronectin type III domain containing 5	Mm01181543_m1
Hgf	Hepatocyte growth factor	Mm01135184_m1
Igf1	Insulin like growth factor 1	Mm00439560_m1
Igf2	Insulin like growth factor 2	Mm00439564_m1
Lama2	Laminin subunit α 2	Mm00550083_m1
Lif	Leukemia inhibitory factor	Mm00434762_g1
Mmp2	Matrix metallopeptidase 2	Mm00439498_m1
Mmp9	Matrix metallopeptidase 9	Mm00442991_m1
Mmp14	Matrix metallopeptidase 14	Mm00485054_m1
Myf5	Myogenic factor 5	Mm00435125_m1
Myod1	Myogenic differentiation 1	Mm00440387_m1
Myog	Myogenin	Mm00446194_m1
Ngf	Nerve growth factor	Mm00443039_m1
Ntf3	Neurotrophin 3	Mm00435413_s1
Pax3	Paired box 3	Mm00435491_m1
Pax7	Paired box 7	Mm01354484_m1
Pparg	Peroxisome proliferator activated receptor-γ	Mm00440940_m1
Tcf4	Transcription factor 4	Mm00443210_m1
Timp1	TIMP metallopeptidase inhibitor 1	Mm01341361_m1
Timp2	TIMP metallopeptidase inhibitor 2	Mm00441825_m1
Vegfa	Vascular endothelial growth factor A	Mm00437306_m1
Zfp423	Zinc finger protein 423	Mm00677660_m1

the transcript sequences from Gencode's GRCm38, release M17. The percentage of reads mapped to the transcriptome ranged from 35.65 to 47.26%. To investigate why Salmon was unable to map large percentages of reads, we performed traditional genome alignment on all reads using STAR (version 2.5.3a) to count the number of reads that did not map anywhere to the genome. To estimate the number of intronic reads, we used a modified gtf file designating the intron regions and featureCounts from Subread (version 1.5.2) with –fracOverlap 0.51 to only count reads that had at least 50.1% of their length aligned within introns. The number of intergenic reads was estimated by subtracting off the numbers of unaligned reads and intronic reads from the number of reads Salmon failed to map to the transcriptome. The number of reads Salmon did align to the transcriptome (17.5–23.7 million in each sample) was still sufficient for the statistical analysis. Files were uploaded to the Gene Expression Omnibus database (accession number GSE122628).

Pericyte Differentiation Assays

For evaluation of myogenic differentiation, $CD146^+Lin^-$ and $NG2^+Lin^-$ pericytes were isolated from nonstimulated muscles (6 donor mice, 12 gastrocnemius-soleus complexes per pericyte type) as described above and grown to 100% confluence in Dulbecco's modified Eagle's medium (DMEM) with 4.5 g/L L-glutamine and sodium pyruvate containing 10% FBS at 37°C, 5% CO_2 with media changes every 3 days. Upon achieving 100% confluence, cells were differentiated in DMEM with 4.5 g/L L-glutamine and sodium pyruvate containing 2% horse serum (HS) at 37°C, 5% CO_2 with media changes every 3 days. Following 30 days of myogenic differentiation, cells were fixed in 4% paraformaldehyde for 30 min at 4°C. The cells were then washed with PBS, blocked for 1 h in 10% horse serum and stained with MF 20 antibody (1:50 dilution, 1% HS) and Alexa Fluor 633 secondary antibody (1:100 dilution, 1% HS). For evaluation of multilineage potential, mouse bone marrow-derived mesenchymal stem cells (BM-MSCs; Passage 26; American Type Culture Collection, Manassas, VA) served as positive controls (seeded at ~33×10^3 cells/well on six-well laminin-coated BioFlex culture plates). Pericytes and BM-MSCs were placed in StemXVivo Osteogenic/Adipogenic Base Media (R&D Systems, Minneapolis, MN) for 48 h and then expanded to the desired level of confluence in DMEM with 4.5 g/L L-glutamine and sodium pyruvate containing 10% FBS at 37°C, 5% CO_2. For osteogenic differentiation, cells were grown to 70% confluence and medium was changed to StemXVivo Osteogenic/Adipogenic Base Media containing StemXVivo Osteogenic Supplement (R&D Systems) ($n = 3$). Medium was changed every 3 days. Following 16 days of osteogenic differentiation, cells were fixed with 4% paraformaldehyde for 1 h at room temperature. The cell layer was washed twice with PBS and stained with 2% (wt/vol) Alizarin Red S (Sigma-Aldrich, St. Louis, MO) solution for 2 min. For adipogenic differentiation, cells were grown to 100% confluence and medium was changed to StemXVivo Osteogenic/Adipogenic Base Media containing StemXVivo Adipogenic Supplement (R&D Systems) ($n = 3$). Medium was changed every 3 days. Following 12 days of adipogenic differentiation, cells were fixed with 4% paraformaldehyde for 1 h at room temperature. The cell layer was washed twice with PBS and once with 60% isopropanol and then stained with working Oil Red O solution for 5 min. Cells were washed four times with distilled H_2O. Cells were imaged using a light microscope (Axiovert 200; Carl Zeiss) with accompanying camera (AxioCam MRc; Zeiss) and software package (AxioVs40 version 4.8.2.0).

In Vitro Mechanical Strain

$CD146^+Lin^-$ and $NG2^+Lin^-$ pericytes were isolated from nonstimulated muscles as described above and expanded to 90% confluence on uncoated plastic tissue culture dishes. After a 1-wk recovery and expansion period, each cell type was detached using Accutase enzyme solution (Millipore Sigma) and seeded onto two, six-well laminin-coated BioFlex culture plates (Flexcell International, McKeesport, PA; 10×10^4/well for $CD146^+Lin^-$ and 30×10^3/well for $NG2^+Lin^-$ cells; $n = 6$ unstrained; $n = 6$ strained). Cells were incubated in 1× high glucose DMEM with 10% FBS and 1% P/S for 3–4 days to allow for sufficient cell attachment. After 3–4 days, cells were washed with PBS and switched to serum-free high glucose DMEM. Equibiaxial mechanical strain (10%, 1 Hz) was applied to cells for 1 h using a FX-4000 Flexercell strain unit (Flexcell International) (25). Cells maintained under static conditions were used as unstrained controls. To determine if strain was an essential requirement for myogenesis, the differentiation experiment described above was repeated following nonstrain and strain conditions. In a separate experiment, conditioned medium was collected from both pericyte types 24 h poststrain. C_2C_{12} cells were grown in DMEM with 4.5 g/L L-glutamine and sodium pyruvate containing 10% FBS at 37°C, 5% CO_2 with media changes every 3 days. Upon achieving 100% confluence, cells were differentiated in DMEM with 4.5 g/L L-glutamine and sodium pyruvate containing 2% HS at 37°C, 5% CO_2 with media changes every 3 days until myotubes were fully formed. Conditioned media from each pericyte type (unstrained conditioned medium was pooled and applied to myotubes, strained conditioned medium was pooled and applied to myotubes) were added to each well containing C_2C_{12}-derived myotubes ($n = 4$), and then images of myotubes were obtained at 24 h and myotube diameter was evaluated using Photoshop CS5. Each myotube was measured in 3 distinct nonoverlapping areas to determine the mean diameter and up to 100 myotubes were measured per well.

Pericyte Transplantation and Training Study

$CD146^+Lin^-$ pericytes were isolated from four donor animals (8 quadricep, 8 TA and 8 gastrocnemius-soleus complexes in total) as

described above and expanded to 90% confluence on uncoated plastic tissue culture dishes (~1 wk). Pericytes were bilaterally injected into TA (~25,000 cells in 20 μL PBS) and gastrocnemius (~40,000 cells in 40 μL PBS) muscles of 4-mo-old mice ("$CD146^+$"). Cells were distributed longitudinally across the muscle as the syringe was removed. A separate group of mice were unilaterally injected with PBS as a control ("PBS"). A third group of mice received no treatment ("Control"; no injection, no e-stim). Pericyte and PBS injected mice were subjected to unilateral e-stim immediately postinjection as described above. Mice received e-stim treatment a total of 2 days/wk, for a total of 4 wk (8 sessions total). Twenty-four hours following the final stimulation, muscles were weighed and rapidly frozen in liquid nitrogen-cooled isopentane and stored at −80°C.

Skeletal Muscle Immunofluorescence and Image Analyses

Transverse sections (10 μm nonserial, separated by at least 50 μm) were obtained for immunofluorescence analyses. Muscle sections were fixed in ice-cold acetone for 15 min and washed with 1× PBS. Sections were blocked for 1 h at room temperature with AffiniPure Fab Fragment goat anti-mouse IgG (H^+L) (55 μg/mL, no. 115-007-003; Jackson ImmunoResearch Laboratories, West Grove, PA) in 5% bovine serum albumin (BSA) and 0.05% Tween 20 in 1× PBS. Primary and secondary antibodies were applied for 1 h, and then, sections were stained with 4′,6-diamidino-2-phenylindole (DAPI; 1:20,000; Sigma-Aldrich) to identify nuclei. To assess myofiber cross-sectional area (CSA) and muscle capillarization, sections were incubated with rat anti-mouse CD31 (Clone 390) (1:100; no. 14-0311-82; Thermo Fisher Scientific) and rabbit anti-mouse dystrophin (1:100; Abcam, Cambridge, MA; ab15277). Fiber type-specific CSA was also evaluated using mouse IgG2b monoclonal anti-type 1 MHC (clone BA-D5, 1:20), mouse IgG1 monoclonal anti-type 2a MHC (clone SC-71, 1:50), mouse IgM monoclonal anti-type 2b MHC (clone BF-F3, 1:50), and mouse IgM monoclonal anti-type 2× MHC (clone 6H1, 1:20) antibodies (Developmental Studies Hybridoma Bank, Iowa City, IA). To assess collagen accumulation, sections were incubated with rabbit anti-mouse collagen type I (1:100; ; ab34710; Abcam). To assess ECM remodeling, sections were incubated with collagen hybridizing peptide (F-CHP) (20 μM concentration, 3Helix, no. FLU300). TA F-CHP content was quantified using a threshold intensity program from ImageJ. For all analyses, tissue sections were visualized using an inverted fluorescent microscope and five random images were acquired at 20X magnification with a Zeiss Axiocam digital camera and Axiovision software (Zeiss, Thornwood, NY). To quantify myofiber CSA, images were imported into Adobe Photoshop (CS5 Extended) and a minimum of 200 fibers were circled using the magnetic lasso tool. Muscle capillarization was assessed as described previously (25). TA collagen content was quantified with a threshold intensity program from ImageJ. RGB channels were separated, and then, the red channel threshold was set to remove background to determine the percentage of collagen observed within each imaged muscle section.

Statistical Analysis

Data are presented as means ± SE. To determine significance, comparisons between groups were evaluated by either an unpaired *t* test (acute e-stim flow cytometry and gene expression experiments), one-way ANOVA (pericyte transplantation and training experiment), or two-way ANOVA (myotube diameter experiment). For myotube diameter, a two-way repeated measures ANOVA with time (pre vs. post) as repeated measures (or within-subjects) factor and treatment as between subjects factor was completed. Data were considered significant at $P \leq 0.05$. All calculations were performed with GraphPad Prism statistical software (6.0; GraphPad Software, San Diego, CA). For the RNA-Seq experiment, TMM normalization (41) was performed to adjust for biases in RNA composition. The detection threshold was set ≥ 0.5 counts/min in ≥ 3 samples, resulting in the filtering of 27,353 genes and leaving 26,363 genes to be analyzed for differential expression. Surrogate variable analysis (29, 30) was performed to remove or control unknown/batch effects that might obscure the detection of DE. DE analysis between unstimulated (sham) and stimulated pericytes (e-stim) was performed using edgeR's quasi-likelihood pipeline (10). False discovery rate (FDR) correction was used; because only one gene met the traditional threshold of < 0.05, we increased the "significance" threshold to 0.5 to assess a larger list of genes that showed the most evidence for differential expression, albeit at a higher false positive rate.

RESULTS

Muscle-Resident Interstitial Cell Quantity Is Not Altered Following Acute Contraction

Characterization of force output and extent of muscle fatigue during an acute bout of e-stim is provided in Supplemental Fig. S1 (all Supplemental Material is available at https://doi.org/10.6084/m9.figshare.9693524.v1). Figure 1, *A* and *B*, illustrates the gating of various mononuclear cell populations in skeletal muscle following an acute bout of e-stim, including $NG2^+$ and $CD146^+$ pericytes, $PDGFR^+$ FAPs, and the combined CD45/CD31 hematopoietic and endothelial cell fraction (abbreviated Lineage Positive or "Lin"). Two subpopulations of mononuclear cells were evident for $CD146^+$ cells, including one population that exhibited low expression and another that exhibited high expression for CD146 (data not shown). $CD146^{+Hi}$ and $CD146^{+Lo}$ cells were evaluated together as one population. The relative baseline percentages of each mononuclear cell population are reported after exclusion of Lin^+ cells: 5.5 ± 1.6% for $NG2^+Lin^-$ cells, 57.4 ± 6.5% for $CD146^+Lin^-$ cells, and 13.5 ± 2.6% for $PDGFR\alpha^+Lin^-$ cells (Fig. 1*C*). The relative quantity of mononuclear cells did not change 24 h following an acute bout of e-stim (Fig. 1*C*). However, a nonsignificant trend toward an increase in the percentage of $CD146^+Lin^-$ ($P = 0.0658$) pericytes was observed following acute e-stim compared with sham controls (Fig. 1*C*).

Multiplex flow cytometry was also used to assess changes in cell surface marker expression as a result of muscle contraction (Fig. 1, *D–G*). Lin was minimally expressed by $NG2^+$ (5.3 ± 1.5%) and $PDGFR\alpha^+$ (3.7 ± 1.1%) cells, whereas 46.8 ± 12.1% of CD146 pericytes expressed Lin, under baseline conditions (Fig. 1*D*). Nearly all $NG2^+Lin^-$ pericytes (94.3 ± 1.1%) expressed CD146 (Fig. 1*E*), whereas only 8.7 ± 1.8% of $CD146^+Lin^-$ pericytes expressed NG2 (Fig. 1*F*), suggesting that $NG2^+$ pericytes represent a sub-population of the larger $CD146^+$ pericyte fraction. Whereas 51.3 ± 5.4% of $NG2^+Lin^-$ pericytes expressed PDGFRα (Fig. 2*G*), only 14.1 ± 2.9% of $CD146^+Lin^-$ pericytes expressed PDGFRα (data not shown), suggesting preferential expression of PDGFRα in $NG2^+$ compared with $CD146^+$ pericytes. Acute e-stim did not alter any of these percentages, with the exception of the percentage of NG2 cells expressing CD146, which increased from 94.3 to 97.4% ($P < 0.05$).

Muscle-Resident Interstitial Cells Differentially Respond to Acute Contraction

Muscle resident interstitial cell gene expression was assessed 3 and 24 h following acute contraction (Figs. 2–4). We targeted genes relevant to myofiber repair/growth and

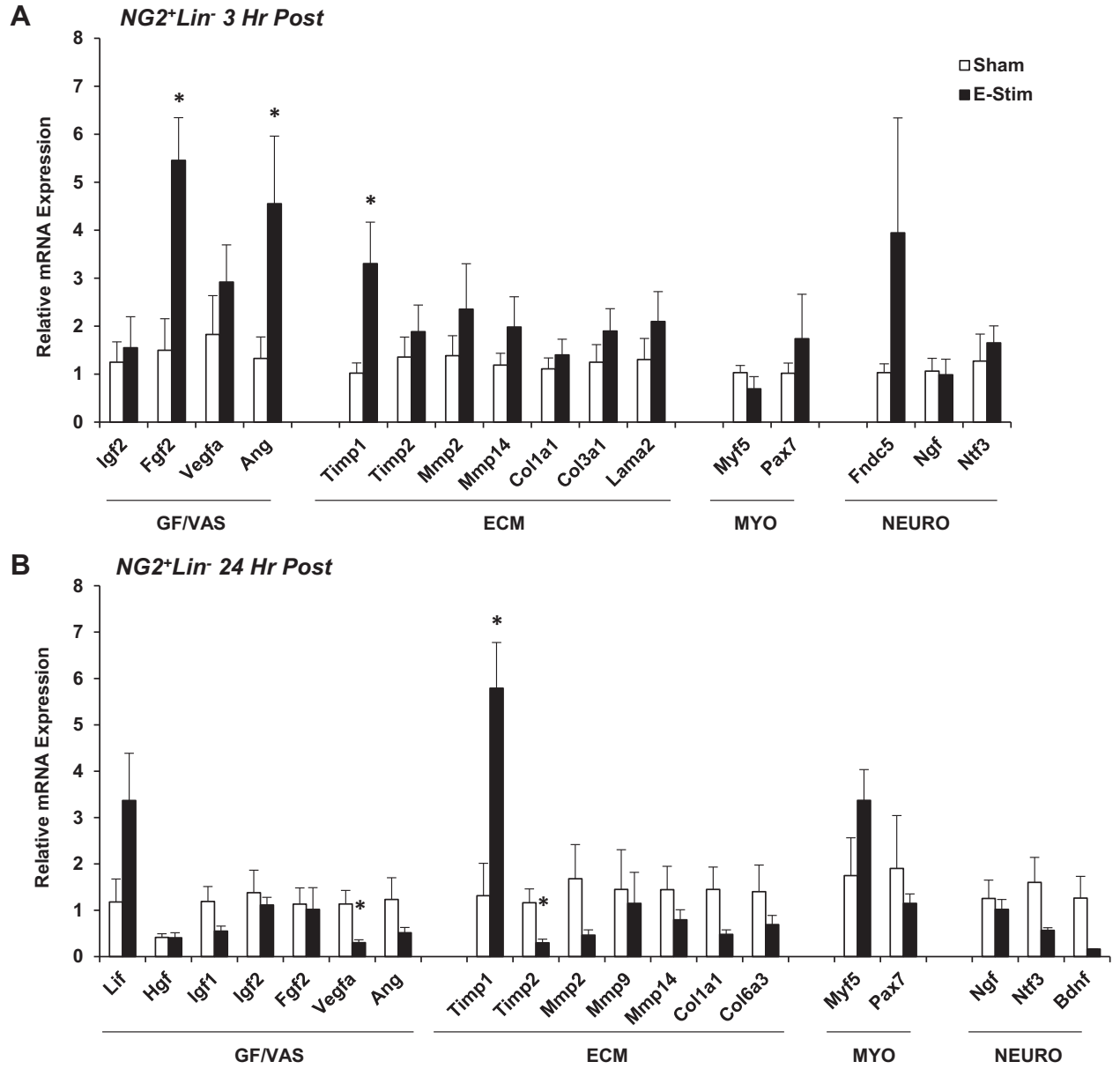

Fig. 2. Impact of muscle contraction on neuron-glial antigen 2-positive lineage-negative ($NG2^+Lin^-$) pericyte gene expression. Mice (15-to 17 wk old) were subjected to a single bout of electrical stimulation (e-stim). Gastrocnemius-soleus complexes were harvested and processed 3 h (*A*) and 24 h (*B*) post e-stim for isolation of pericytes by FACS and targeted analysis of gene expression using quantitative PCR. Genes are categorized by function, including factors related to tissue growth and vascular remodeling (GF/VAS), extracellular matrix remodeling (ECM), myogenesis (MYO), and neurogenic support (NEURO). Values are means ± SE (n = 3–6). *$P < 0.05$ vs. sham.

vascular remodeling (GF/VAS), extracellular matrix remodeling (ECM), myogenesis (MYO), fibroadipogenesis (FA), and nerve repair/neurogenesis (NEURO). Several genes were not expressed in $NG2^+Lin^-$ pericytes under sham conditions or 3 h poststimulation, including leukemia inhibitory factor (*Lif*), hepatocyte growth factor (*Hgf*), epidermal growth factor (*Egf*), matrix metalloproteinase-9 (*Mmp9*), myogenic differentiation 1 (*Myod*), myogenic factor 4 (*Myogenin*), peroxisome proliferator-activated receptor-γ (*Pparg*; adipogenic differentiation), zinc finger protein 423 (*Zfp423*; adipogenic differentiation), and brain-derived neurotrophic factor (*Bdnf*). However, fibroblast growth factor 2 (*Fgf2*) ($P < 0.05$) and angiogenin (*Ang*) ($P < 0.05$) gene expression was significantly increased at 3 h poststimulation, as well as the tissue inhibitor of metalloproteinase-1 (*Timp1*) ($P < 0.05$) (Fig. 2*A*). Myogenic (*Myod* and *Myogenin*) and adipogenic (*Pparg*) gene expression remained unamplified and Timp1 ($P < 0.05$) was sustained at 24 h poststimulation (Fig. 2*B*).

Similar to $NG2^+Lin^-$ pericytes, *Fgf2* gene expression was increased in $CD146^+Lin^-$ pericytes at 3 h poststimulation ($P = 0.05$), as well as several genes related to ECM remodeling, including *Timp1* ($P < 0.05$), *Timp2* ($P = 0.05$), *Mmp2* ($P = 0.05$), *Mmp14* ($P < 0.05$), and collagen type 1, α1 *(Col1a1)* ($P < 0.05$) (Fig. 3*A*). Nerve growth factor (*Ngf*) was also increased at 3 h poststimulation ($P < 0.05$). While most ECM-related gene expression returned to sham values

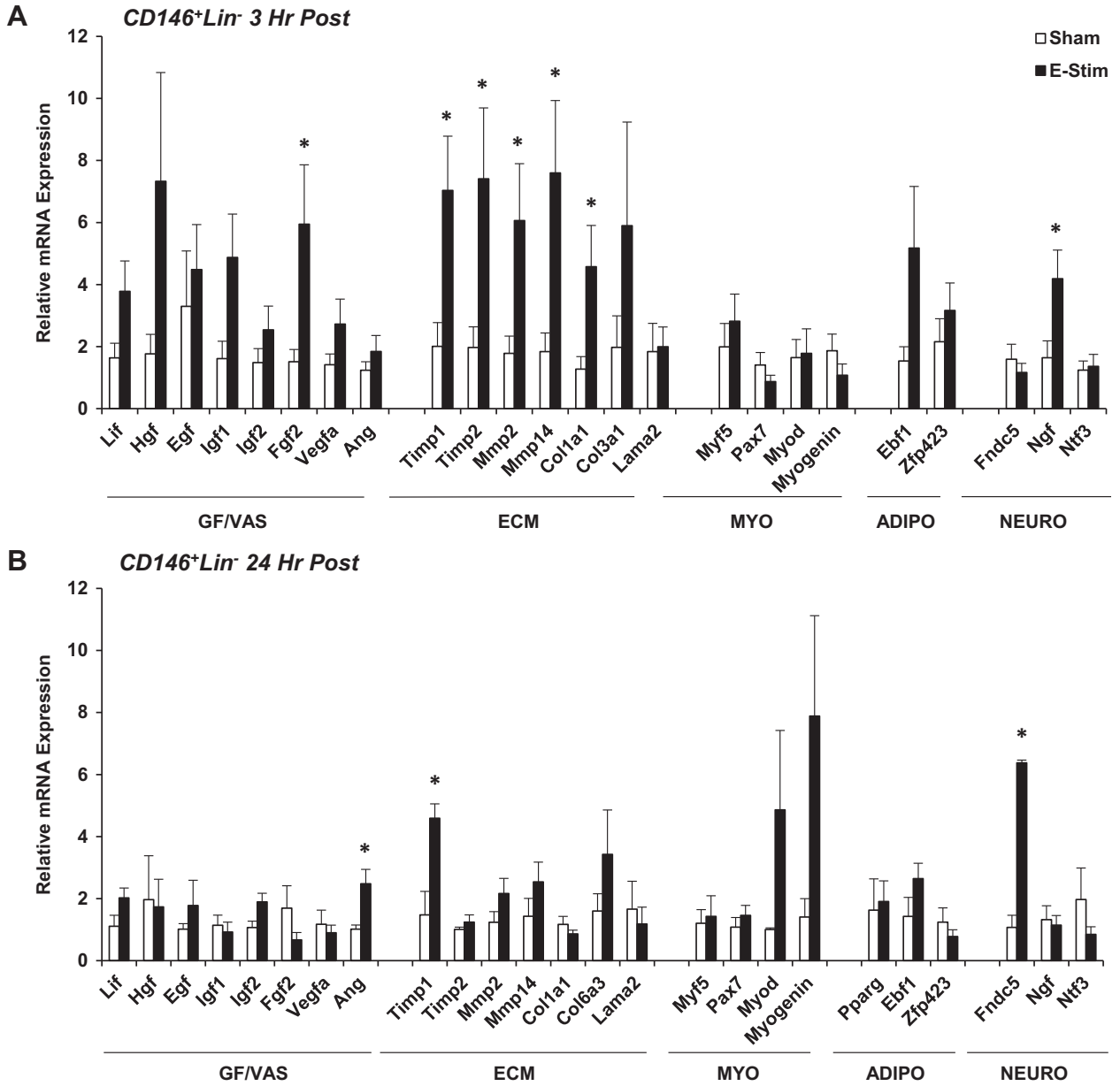

Fig. 3. Impact of muscle contraction on CD146$^+$Lin$^-$ pericyte gene expression. Mice (15-to 17 wk old) were subjected to a single bout of electrical stimulation (e-stim). Gastrocnemius-soleus complexes were harvested and processed 3 h (*A*) and 24 h (*B*) post e-stim for isolation of pericytes by FACS and targeted analysis of gene expression using quantitative PCR. Genes are categorized by function, including factors related to tissue growth and vascular remodeling (GF/VAS), extracellular matrix remodeling (ECM), myogenesis (MYO), adipogenesis (ADIPO), and neurogenic support (NEURO). Values are means ± SE (n = 3–6). *$P \leq 0.05$ vs. sham.

at 24 h poststimulation, *Ang* ($P < 0.05$) and fibronectin type III domain-containing protein 5 (*Fndc5*) ($P < 0.05$) increased 24 h poststimulation (Fig. 3*B*). Adipogenic gene expression (*Pparg*, early B cell factor-1 [*Ebf1*], *Zfp423*) was detected in CD146$^+$Lin$^-$ pericytes but not significantly altered at either time point poststimulation (Fig. 3*B*).

Very few genes amplified or were differentially regulated in PDGFRα^+Lin$^-$ FAPs at 3 or 24 h poststimulation (Fig. 4, *A* and *B*). Variability in gene expression was high at both time points. The exception was that both *Ebf1* and *Zfp423* were downregulated with stimulation, and a significant decrease was detected for *Ebf1* gene expression at 24 h ($P < 0.05$; Fig. 4*B*). These data are consistent with previous in vitro data that demonstrate the ability for mechanical strain to inhibit adipogenic gene expression in mesenchymal stem cells (44). Transcription factor 4 (*Tcf4*), a fibroblast marker, was also significantly decreased as a result of acute e-stim ($P < 0.05$) (Fig. 4*B*).

Contraction Stimulates Muscle-Resident CD146$^+$Lin$^-$ Pericytes to Synthesize RNAs that Regulate the Immune System and ECM Remodeling

The results from targeted gene expression analyses suggested that CD146$^+$Lin$^-$ pericytes were highly responsive to the stimulus of acute contraction. To further elucidate the

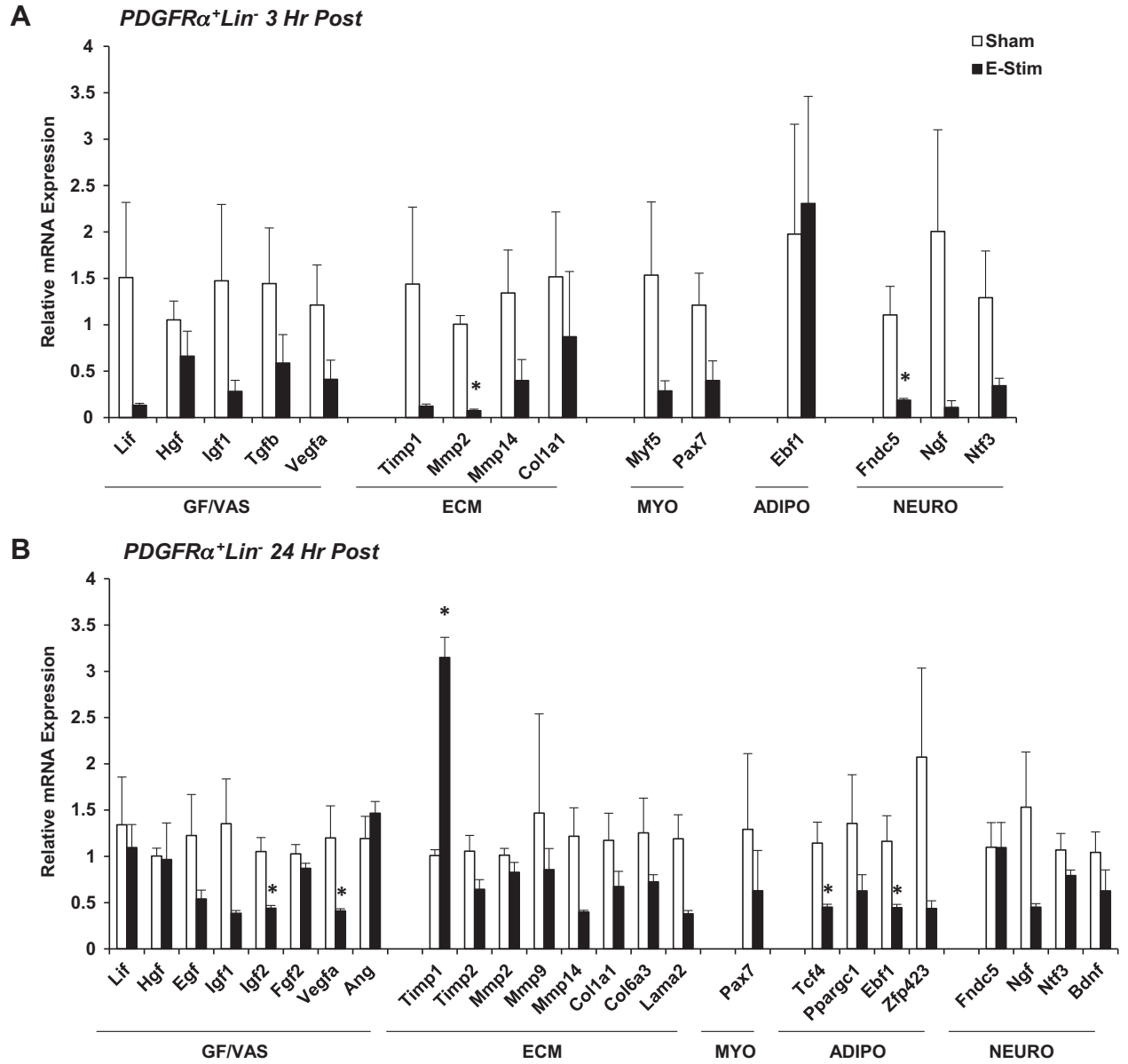

Fig. 4. Impact of muscle contraction platelet-derived growth factor receptor-α-positive lineage-negative (PDGFα$^+$Lin$^-$) fibroadipogenic progenitor (FAP) cell gene expression. Mice (15-to 17 wk old) were subjected to a single bout of electrical stimulation (e-stim). Gastrocnemius-soleus complexes were harvested and processed 3 h (*A*) and 24 h (*B*) post e-stim for isolation of FAPs by FACS and targeted analysis of gene expression using quantitative PCR. Genes are categorized by function, including factors related to tissue growth vascular remodeling (GF/VAS), extracellular matrix remodeling (ECM), myogenesis (MYO), fibroadipogenesis (ADIPO), and neurogenic support (NEURO). Values are means ± SE (n = 3–6). *$P < 0.05$ vs. sham.

CD146$^+$Lin$^-$ pericyte response to acute contraction, RNA sequencing (RNA-Seq) was performed on CD146$^+$Lin$^-$ pericytes isolated from sham controls (unstimulated) and mice 3 h following an acute bout of e-stim. The percentage of reads aligned to the transcriptome ranged from 35.7 to 47.3% (data not shown), which is lower compared with other RNA-Seq experiments on mouse (usually 90%). Traditional genomic alignment showed that 13.1 to 29.6% did not align anywhere in the genome, 25.9 to 33.2% aligned within introns and 4.8–14.0% aligned between genes. The high percentage of intronic reads suggests an abundance of pre-mRNAs due to a high rate of transcription (1). The unmapped reads were discarded before further analysis. Using a modified FDR rate of 0.5, 329 genes were differentially expressed as a result of e-stim (Fig. 5). A total of 172 genes were upregulated by contraction, including genes important for adhesion and migration (*Ccl17*, *Thbs1*, *Ccl7*, *Sned1*, *Ccr7*, *Selp*, and *Ncam*), immunomodulation (*Il1rn*, *Ptx3*, *Cxcl3*, *Ccl17*, *Hmox1*, *Lcn2*, *Acod1*, *Tlr13*, *Cxcl2*, *Csf1*, *Ccr1*, *Il1b*, *Trem1*, *Lilrb4*, *S100a9*, *Ccl7*, *Cxcr5*, *Lilrb4a*, *Lifm*, *S100a8*, *Ltf*, *Il33*, *Cd14*, *Il1r2*, *Il5*, *Ackr2*, and *Csf3r*), ECM remodeling (*Ptx3*, *Fgl2*, *Serpine1*, *Col18a1*, *Mmp8*, *Adamts4*, *Mmp19*, *Thbs1*, and *Mmp14*), and angiogenesis (*Thbs1*). In contrast, 157 genes were downregulated by contraction, including genes that control cellular proliferation (*Fos*, *Fosb*, *Src*, *Egr3*, and *Prc1*). A list of the top 25 differentially expressed genes is presented in Table 2.

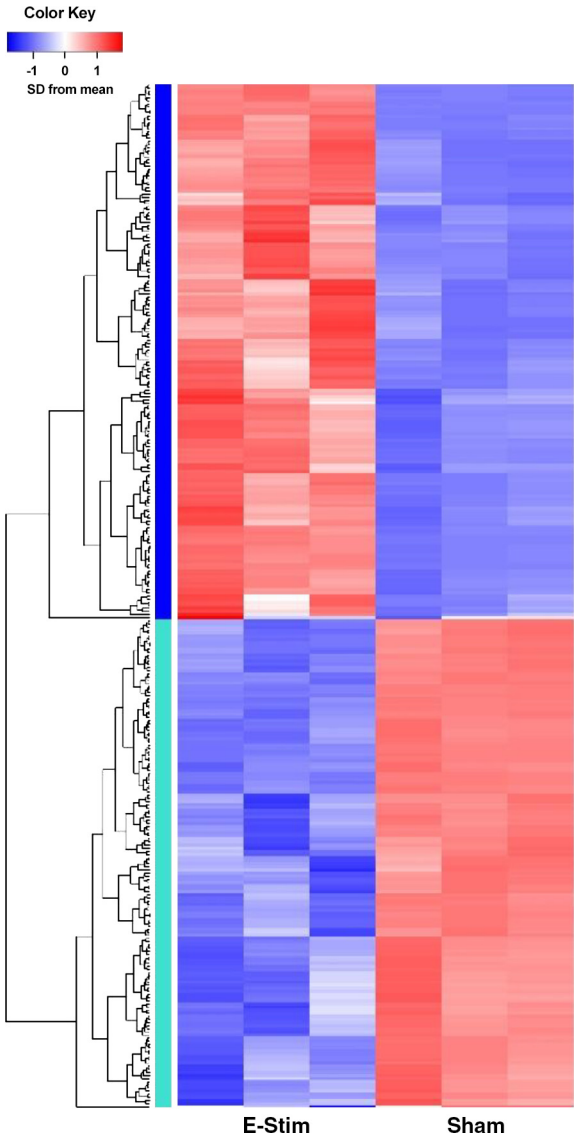

Fig. 5. Muscle-derived CD146$^+$Lin$^-$ pericytes synthesize RNAs that regulate extracellular matrix (ECM) remodeling and the immune system following muscle contraction. Mice (15-to 17 wk old) were subjected to a single bout of electrical stimulation (e-stim; $n = 3$ per group). Hindlimb muscles were harvested and processed 3 h post e-stim for isolation of CD146$^+$Lin$^-$ by FACS and RNA-sequencing (RNA-seq). RNA-Seq libraries were prepared and sequenced on a HiSeq 4000. Salmon (version 0.8.2) was used to quasi-map reads to the transcriptome. 329 genes were differentially expressed by pericytes following muscle contraction (E-Stim) compared with control conditions (Sham) using a modified false discovery rate of 0.5.

Muscle-Derived CD146$^+$Lin$^-$ Pericytes Secrete Factors in Response to In Vitro Mechanical Strain that Positively Influence Myotube Growth

During recovery from FACS, adherent NG2$^+$Lin$^-$ and CD146$^+$Lin$^-$ pericytes were evaluated daily for morphology by bright-field microscopy. Morphological differences were evident. CD146$^+$Lin$^-$ pericytes exhibited a traditional fibroblast-like structure, whereas NG2$^+$Lin$^-$ remained punctate (Fig. 6*A*). Despite prior reports that pericytes possess myogenic potential in culture and in vivo (4, 42), neither pericyte type formed myotubes or positively stained for myosin heavy chain following exposure to differentiation media, even after extended incubation (30 days) (data not shown). CD146$^+$Lin$^-$ pericytes were also subjected to an acute bout of in vitro mechanical strain using a Flexcell system before differentiation, but stimulation similarly failed to initiate myotube formation (data not shown). Muscle-resident CD146$^+$Lin$^-$ pericytes also did not exhibit adipogenic or osteogenic potential on standard plastic culture dishes. BM-MSCs served as controls for these experiments and appropriately differentiated into adipocytes and osteocytes under nonstrained conditions, as confirmed by the presence of lipid vacuoles and calcium deposits, respectively (Fig. 6*B*). In BM-MSC-positive controls, ~40% of cells within each well displayed red-stained lipid droplets, while 80–90% of each well exposed to osteogenic differentiation media stained positive for mineralization with Alizarin Red S.

To evaluate the capacity for pericytes to influence myofiber growth via secretion of paracrine factor, NG2$^+$Lin$^-$ and CD146$^+$Lin$^-$ pericytes were isolated by FACS, recovered on plastic culture dishes for 1 wk, transferred to dishes compatible with a Flexcell system (laminin-coated silicone membranes), and subjected to a single bout of mechanical strain (Fig. 6*C*). NG2$^+$Lin$^-$ conditioned media did not alter myotube diameter (Fig. 6*D*). In contrast, addition of strained conditioned media from CD146$^+$Lin$^-$ cells significantly increased myotube diameter (time $\times$ treatment interaction, $P = 0.06$; time main effect, $P < 0.05$; treatment main effect, $P < 0.05$; Fig. 6, *E* and *F*).

Muscle-Derived CD146$^+$Lin$^-$ Pericytes Contribute to Skeletal Muscle Remodeling in Response to Training

Overall, CD146$^+$Lin$^-$ pericytes demonstrated the greatest capacity for induction of muscle growth in response to contraction. Thus an in vivo injection study was conducted to

Table 2. *Top 25 differentially expressed genes*

Gene Symbol	Fold Change	FDR *P* Value
Kcnh3	−17.1932	0.018404
Kcnd3	−13.9631	0.05408
Mt1	5.447944	0.06271
Ighg3	−14.7743	0.123321
Il1rn	5.489686	0.135965
Gm2026	34.35529	0.135965
Fosb	−2.97013	0.135965
Rasgef1b	−3.02143	0.135965
Map3k6	4.117265	0.135965
Zbtb16	5.436701	0.135965
Kbtbd11	3.145345	0.135965
Fkbp5	4.333237	0.135965
Gm15927	6.509305	0.135965
Ptx3	11.05306	0.135965
Akap12	2.664333	0.135965
Cxcl3	9.384394	0.141689
Ccl17	9.327709	0.141689
Gm10714	−4.33978	0.141689
Mt2	14.93578	0.159589
Fras1	−6.73273	0.159589
Thbs1	3.428286	0.159589
Rpl34-ps1	−5.77996	0.159589
Hmox1	5.773782	0.159589
Dock3	−4.48992	0.159589

FDR, false discovery rate.

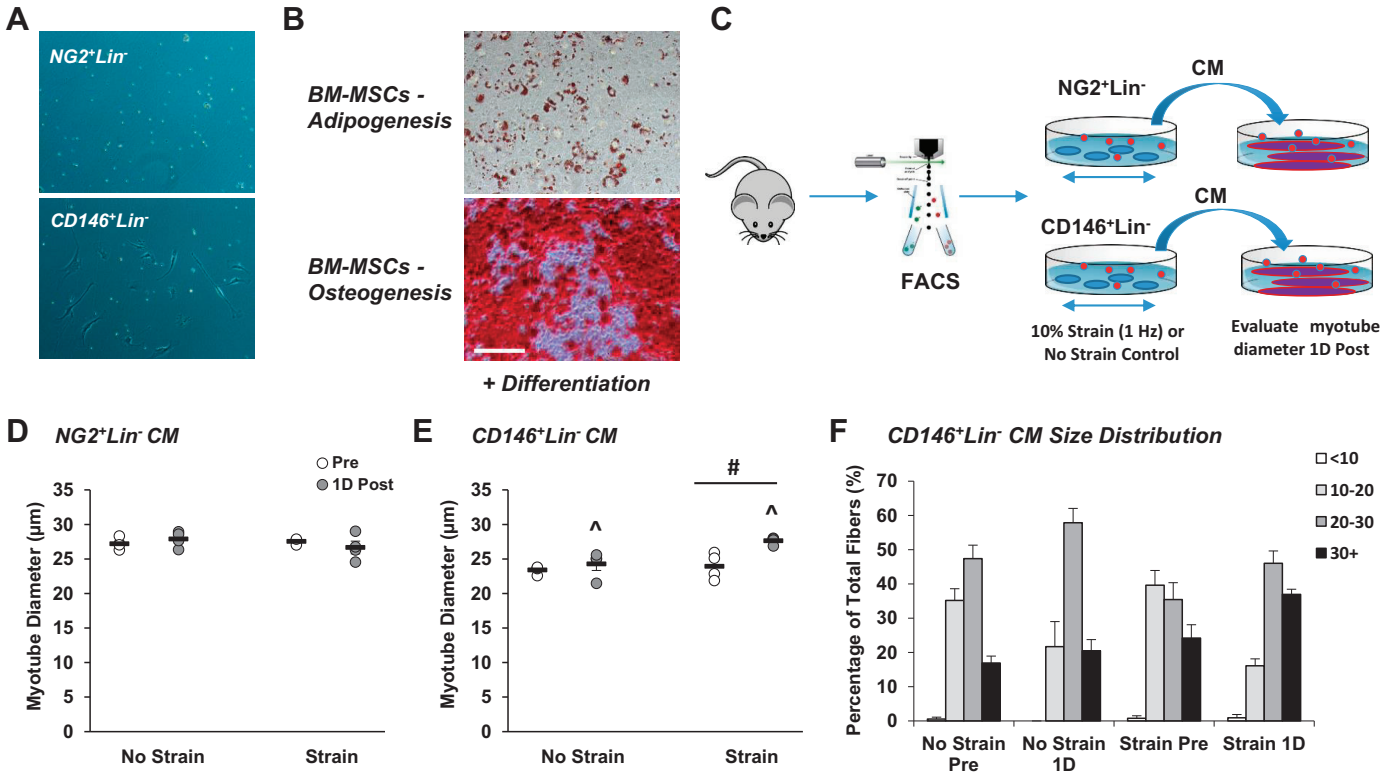

Fig. 6. Muscle-derived CD146$^+$Lin$^-$ pericytes secrete factors in response to in vitro mechanical strain that positively influence myotube growth**.** Neuron-glial antigen 2-positive lineage-negative (NG2$^+$Lin$^-$) and CD146$^+$Lin$^-$ pericytes were isolated from unstimulated mouse muscle by fluorescence-activated cell sorting. *A*: morphology of pericytes after 1 wk in culture. Whereas NG2$^+$Lin$^-$ pericytes demonstrate a punctate shape, CD146$^+$Lin$^-$ pericytes exhibit a fibroblast-like morphology. *B*: pericytes and bone marrow-derived MSCs (BM-MSCs) were plated on plastic culture dishes and evaluated for differentiation capacity. Pericytes did not demonstrate capacity for myogenesis, adipogenesis, or osteogenesis (not shown). Control BM-MSCs display capacity for adipogenesis based on Oil Red O Staining (*top*) and osteogenesis based on Alizarin Red S staining (*bottom*); $n = 3$. *C*: muscle-resident pericytes were subjected to a single bout of in vitro mechanical strain using a Flexcell System (laminin-coated plates, 10% strain, 1 Hz, 1 h). FACS, fluorescence-activated cell sorting. *D* and *E*: 24 h following in vitro mechanical strain, pericyte-derived conditioned media (CM; strained or no strain control) was collected and subsequently added to mature myotubes in culture. Whereas addition of NG2$^+$Lin$^-$ CM did not influence myotube growth (*D*), CD146$^+$Lin$^-$ CM significantly increased myotube growth (*E*) at 1 day (1D) postincubation. *F*: myotube size distribution is provided for cells exposed to CD146$^+$Lin$^-$ conditioned media. ^ Time main effect, $P < 0.05$; #treatment main effect, $P < 0.05$. Values are means ± SE ($n = 4$).

assess their contribution to adaptation and remodeling in response to training. CD146$^+$Lin$^-$ pericytes were bilaterally transplanted into TA and gastrocnemius muscle and subsequently subjected to 4 wk of of electrical stimulation (Fig. 7*A*). Pericyte transplantation did not significantly increase the mean fiber CSA compared with controls (Fig. 7*B*), yet a trend was noted for an increase in the percentage of fibers ranging greater 3,000 μm^2 in the TA muscle ($P = 0.058$) (Fig. 7*C*). No significant differences in mean fiber CSA were detected in the TA based on fiber type (Supplemental Fig. S2*A*). In the gastrocnemius muscle, a trend for an increase in the mean fiber CSA was detected ($P = 0.108$; Supplemental Fig. S2*B*). ECM remodeling was assessed in the TA by detection of total collagen and degraded collagen (Fig. 7, *D* and *E*). While no differences were noted in total collagen content between groups (Fig. 7*D*), collagen degradation was significantly increased in muscles that received pericyte transplantation ($P < 0.05$; Fig. 7*E*). Capillary density and the capillary:fiber ratio were also increased with pericyte transplantation compared with controls (Fig. 7, *F* and *G*; $P < 0.05$). In addition, the difference in peak torque between the beginning and end of study was significantly increased with pericyte treatment compared with controls (Fig. 7*H*; $P < 0.05$).

DISCUSSION

It is well established that repeated bouts of resistance exercise lead to beneficial structural and functional gains in human skeletal muscle, such as myofiber hypertrophy and increased strength (13). The current study was designed to evaluate muscle-resident interstitial cell responses to an electrical stimulation protocol that replicates resistance exercise and subsequently assess a role for pericytes in skeletal muscle adaptation. While no changes were noted in relative cell quantity following acute e-stim, cellular function based on gene expression was differentially regulated. Notably, CD146$^+$Lin$^-$ pericytes were sensitive to acute contraction and demonstrated enhanced potential for engagement in ECM remodeling, angiogenesis, and immunomodulation following contraction. In vivo transplantation studies in combination with repeated sessions of contraction suggest an important role for CD146$^+$Lin$^-$ pericytes in adaptation, including increased ECM remodeling, vascular growth, and strength. Thus this study provides the first demonstration that CD146$^+$Lin$^-$ pericytes are responsive to muscle contraction and may subsequently contribute to exercise-mediated skeletal muscle adaptation.

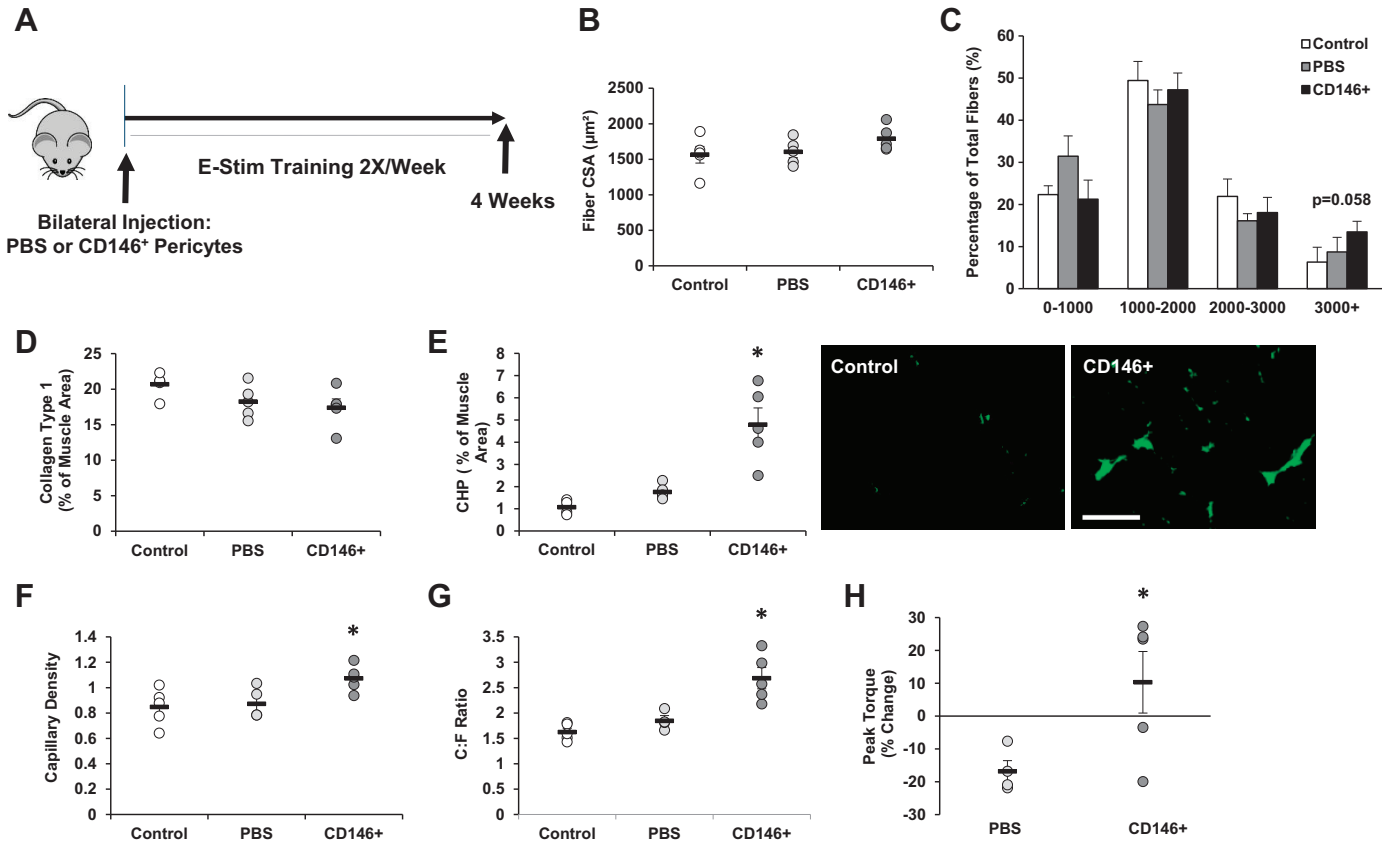

Fig. 7. Muscle-derived CD146$^+$Lin$^-$ pericytes contribute to skeletal muscle remodeling in response to training. *A*: experimental design for CD146$^+$ pericyte transplantation and training study. CD146$^+$Lin$^-$ pericytes were isolated from unstimulated mouse hindlimb muscle by fluorescence-activated cell sorting. Pericytes were bilaterally injected into tibialis anterior (TA) and gastrocnemius muscles of 16-wk-old mice ("CD146$^+$"). A separate group of mice were injected with PBS as a control ("PBS"). A third group of mice received no treatment ["Control"; no injection, no electrical stimulation (e-stim)]. Pericyte and PBS-injected mice were exposed to unilateral e-stim immediately postinjection. E-stim treatment was applied 2 days/wk, for a total of 4 wk (8 sessions total). Twenty-four hours following the final stimulation, muscles were harvested and prepared for immunofluorescence analysis. *B–H*: the following analyses are reported for the TA muscle: mean fiber cross-sectional area (CSA; *B*), minimum 200 fibers analyzed per section, fiber size distribution (*C*), collagen type 1 content (*D*), collagen degradation based on collagen hybridizing peptide (CHP) assay (*E*), capillary density (*F*), capillary to fiber ratio (C:F; *G*), and change in peak torque (*H*) from beginning to end of study. Values are means ± SE ($n = 6$). *$P < 0.05$ vs. Control and PBS.

NG2 and CD146 are integral cell surface proteins that are expressed by a variety of mononuclear cell types in muscle, including endothelial cells and various immune cells (2, 7). Thus a sorting strategy was optimized in this study to isolate muscle-resident interstitial cells after exclusion of CD31$^+$ endothelial and CD45$^+$ hematopoietic/immune cells (designated as the lineage/Lin negative fraction). Exclusion of both CD31 and CD45 on the same channel does not allow estimation of individual endothelial cell or immune cell quantity or the individual relative percentage expression within each pericyte fraction, yet combining does prevent spectral overlap commonly associated with multiplexing. Regardless of this minor limitation, minimal expression of CD31/CD45 in NG2$^+$ pericytes and PDGFRα$^+$ FAPs was confirmed and the relative percentage of both populations in skeletal muscle was low (<10%). In contrast, high expression of CD31/CD45 was observed in CD146$^+$ cells and the relative percentage of CD146$^+$Lin$^-$ cells was high (~60%), highlighting the need to perform the CD31/CD45 exclusion step before further analysis of CD146$^+$ pericytes. The marked difference in baseline NG2$^+$ and CD146$^+$ pericyte relative percentages prompted us to examine coexpression of the different pericyte cell surface markers, which to our knowledge has not been previously reported. Minimal expression of NG2 was observed in the CD146$^+$Lin$^-$ fraction, yet predominant CD146 expression was observed in the NG2$^+$Lin$^-$ fraction (>90%), suggesting that NG2$^+$ pericytes represent a subfraction of CD146$^+$ pericytes. The relative quantity of each cell population remained stable and was not significantly altered in response to acute muscle contraction. These data are consistent with our prior results in humans, which demonstrated a lack of change in the relative NG2$^+$ cell quantity 24, 48, and 168 h following acute resistance exercise (14).

Significant modification of gene expression was observed for both pericyte types at 3 and 24 h following acute e-stim. Targeted gene expression, rather than use of an unbiased high throughput screen, was initially pursued due to the multiple cell types and time points evaluated in the current study. Genes were chosen based on previously published studies that have established an important role for pericytes in paracrine factor secretion and myogenic differentiation (15, 42, 50, 53). In the current study, paracrine factor gene expression was generally higher in both pericyte types at 3 h postacute e-stim compared with 24 h. For example, *Fgf2* and *Ang* gene expression was significantly increased in NG2$^+$ pericytes, suggesting a role for both in the rapid initiation of exercise-induced arteriogenesis

previously observed in mice (25) or angiogenesis observed in the current study. Several factors associated with ECM remodeling also were markedly upregulated in $CD146^+$ pericytes at this early time point, including *Timp1*, *Timp2*, *Mmp2*, *Mmp14*, and *Col1a1*. In contrast to pericytes, $PDGFR\alpha^+$ FAP gene expression was either nonresponsive (3 h), variable (3 and 24 h), or downregulated (24 h) following acute e-stim. We suspect that variability in FAP gene expression reflects the heterogeneous composition of cell types obtained when isolating based on PDGFRα alone.

RNA sequencing was performed on $CD146^+$ pericytes 3 h post-e-stim to provide deeper insight regarding potential mechanisms by which these cells contribute to beneficial outcomes associated with contraction. Although the results aligned to some extent with targeted qPCR results (*Fgf2*, *Timp1*, *Mmp14*), the RNAs upregulated with e-stim were largely and unexpectedly related to immunomodulation. We noted that a high percentage of these genes influence macrophage recruitment, polarization, and/or phenotype (M1 to M2 transition), including macrophage-colony stimulating factor (*Csf-1*) (24), pentraxin-3 (*Ptx3*) (45), heme oxygenase-1 (*Hmox1*) (37, 52), and lipocalin-2 (*Lcn2*) (27). Muscle-resident $CD146^+$ pericyte synthesis of *Hmox1* has also been reported following hypoxia exposure in vitro (9). The appearance of anti-inflammatory M2 macrophages would facilitate satellite cell differentiation and repair mechanisms that ultimately impact muscle structure and function (49). What is not clear is whether pericyte-derived factors directly influence macrophage polarization or if they initiate ECM remodeling in a manner that can indirectly influence macrophage phenotype. For example, studies have demonstrated direct roles for HMOX-1 and PTX3 in ECM turnover in a variety of damaged tissues (3, 18). Regardless, RNA-Seq results suggest an important role for $CD146^+$ pericytes in ECM remodeling and immune cell regulation.

An elevation in *Timp1* gene expression was detected by targeted gene expression analyses in all interstitial cell types ($NG2^+$ and $CD146^+$ pericytes at 3 and 24 h; FAPs at 24 h). An increase in *Timp1* gene expression post-e-stim was also confirmed in $CD146^+$ pericyte samples used for RNA-Seq via qPCR. Interestingly, *Timp1* gene expression is increased to the highest degree in rat skeletal muscle in response to three days of chronic mechanical loading (8, 33, 47), and a general PDGFR inhibitor can suppress both *Timp1* gene expression and load-induced growth (47). Baseline *Timp1* gene expression is also positively correlated with posttraining strength gains in healthy older adults (16). Although TIMP1 is an inhibitor of matrix metalloproteinases and negative regulator of ECM turnover (6), it can also control vascular remodeling similar to FGF-2 and angiogenin (31, 48, 51). A recent study by Mandel et al. (31) reported significant deficiencies in microvascular content as well as lack of prazosin-mediated arteriogenesis in TIMP1 deficient ($Timp1^{-/-}$) mice. The precise role for TIMP1 in the regulation of skeletal muscle adaptation is not clear. However, pericyte-mediated release of TIMP1 may provide the basis for correlations between baseline capillarity and promotion of muscle mass in humans following strength training (46).

Whereas most genes related to myogenic and adipogenic differentiation were not detected in $NG2^+$ cells, several myogenic transcription factors, including *Myf5*, *Pax7*, *Myod*, and *Myogenin*, were expressed in $CD146^+$ cells and enhanced at 24 h postacute stimulation. These results prompted us to compare the capacity for $CD146^+Lin^-$ pericytes to form myotubes in culture, both in the absence and presence of mechanical strain. $CD146^+$ pericytes did not form myotubes under standard differentiation conditions, even after mechanical strain stimulation or 30 days in culture. During the preparation of this manuscript, Guimarães-Camboa et al. (23), reported lineage of tracing of pericytes based on TBX18, a transcription factor recently found to be uniquely expressed in pericytes and vascular smooth muscle cells. This study reported that pericytes retained their identity throughout the lifespan and contribution to other cell types was not observed in vivo. Our gene expression analyses also suggested that pericytes possess minimal mesodermal differentiation potential, which was consistent with the results of our in vitro experiments. Future lineage tracing experiments using the Tbx18-CreERT2 mouse will be necessary to confirm that pericytes maintain their cellular identity following contraction in vivo.

Our in vitro conditioned media experiment suggested the ability for $CD146^+Lin^-$ pericytes to release paracrine factor in response to mechanical strain that can influence myofiber growth. The results from this experiment prompted us to evaluate the potential for $CD146^+$ pericytes to influence muscle adaptation in vivo. Transplantation of $CD146^+$ pericytes before initiation of a 4-wk training study resulted in significant increases in ECM remodeling, vascular growth, and increased strength compared with control groups. A trend toward an increase in the mean myofiber CSA of the gastrocnemius-soleus muscle was noted ($P = 0.108$), as well as an increase in the percentage of fibers $>3{,}000\ \mu m^2$ within the TA ($P = 0.058$). We recently demonstrated the ability for pericytes encapsulated in hydrogel to recover myofiber CSA following disuse atrophy (34), providing evidence of a role for pericytes in the promotion of muscle growth. Experiments are in progress using a higher cell quantity, as well as novel biomaterials to increase cell viability following transplantation. This study did not determine the precise contribution of $NG2^+$ pericytes to muscle growth. The fact that $NG2^+$ pericytes did not influence myotube diameter in culture does not exclude a role for this pericyte type in contraction-mediated adaptation. However, we decided not to pursue an $NG2^+$ pericyte transplantation experiment given practical issues related to low cell yield and rate of expansion, issues that will need to be considered when developing cell-based therapies.

In conclusion, this study provides the first examination of muscle-resident interstitial cell sensitivity to a mechanical stimulus, including the response of pericytes and FAPs to an acute bout of contraction. Whereas the relative quantity of all cells remained stable 24 h following contraction, unique gene expression profiles were noted. Based on the sensitivity of $CD146^+$ pericytes to acute contraction and their ability to induce myotube growth in vitro, these cells were examined for their ability to facilitate skeletal muscle remodeling when combined with an electrical stimulation training protocol for 4 wk. The results from this study provide the first evidence that $CD146^+$ pericytes may contribute to beneficial outcomes associated with exercise training, including enhanced ECM remodeling and angiogenesis.

ACKNOWLEDGMENTS

The authors thank Dr. Barbara Pilas and the Flow Cytometry Center, as well as Dr. Alvaro Hernandez and the High-Throughput Sequencing and Genotyping Unit, at the Roy J. Carver Biotechnology Center (University of Illinois at Urbana-Champaign) for advice and assistance with FACS, flow cytometry, and RNA-Seq.

GRANTS

This work was supported by the National Institute of Arthritis and Musculoskeletal and Skin Diseases of the National Institutes of Health under award number R01AR072735 (to M. D. Boppart) and partially supported by the National Institute of Neurological Disorders and Stroke under award number R21NS104293 (to M. D. Boppart and J. S. Rhodes). S. Dvoretskiy was supported by the National Institute of Biomedical Imaging and Bioengineering of the NIH under award number T32EB019944 and an American College of Sports Medicine National Aeronautics and Space Administration Space Physiology Research Grant (no. 18-00664). C. Coombs was supported by a Santander Research Scholarship from the University of Brighton (Brighton, UK).

DISCLAIMERS

The content is solely the responsibility of the authors and does not necessarily represent the official views of the NIH.

DISCLOSURES

No conflicts of interest, financial or otherwise, are declared by the authors.

AUTHOR CONTRIBUTIONS

S.D., K.G., M.M., and M.D.B. conceived and designed research; S.D., K.G., M.M., Y.P., Z.S.M., C.C., B.B., G.G., G.W., and I.L. performed experiments; S.D., K.G., M.M., J.D., J.S.R., and M.D.B. analyzed data; S.D., K.G., J.D., J.S.R., and M.D.B. interpreted results of experiments; S.D., J.D., and M.D.B. prepared figures; S.D., J.D., and M.D.B. drafted manuscript; S.D., K.G., M.M., Y.P., Z.S.M., C.C., B.B., G.G., G.W., I.L., J.D., J.S.R., and M.D.B. edited and revised manuscript; S.D., K.G., M.M., Y.P., Z.S.M., C.C., B.B., G.G., G.W., I.L., J.D., J.S.R., and M.D.B. approved final version of manuscript.

REFERENCES

1. **Ameur A, Zaghlool A, Halvardson J, Wetterbom A, Gyllensten U, Cavelier L, Feuk L.** Total RNA sequencing reveals nascent transcription and widespread co-transcriptional splicing in the human brain. *Nat Struct Mol Biol* 18: 1435–1440, 2011. doi:10.1038/nsmb.2143.
2. **Armulik A, Genové G, Betsholtz C.** Pericytes: developmental, physiological, and pathological perspectives, problems, and promises. *Dev Cell* 21: 193–215, 2011. doi:10.1016/j.devcel.2011.07.001.
3. **Barikbin R, Neureiter D, Wirth J, Erhardt A, Schwinge D, Kluwe J, Schramm C, Tiegs G, Sass G.** Induction of heme oxygenase 1 prevents progression of liver fibrosis in Mdr2 knockout mice. *Hepatology* 55: 553–562, 2012. doi:10.1002/hep.24711.
4. **Birbrair A, Zhang T, Wang ZM, Messi ML, Enikolopov GN, Mintz A, Delbono O.** Role of pericytes in skeletal muscle regeneration and fat accumulation. *Stem Cells Dev* 22: 2298–2314, 2013. doi:10.1089/scd.2012.0647.
5. **Boppart MD, De Lisio M, Zou K, Huntsman HD.** Defining a role for non-satellite stem cells in the regulation of muscle repair following exercise. *Front Physiol* 4: 310, 2013. doi:10.3389/fphys.2013.00310.
6. **Brew K, Nagase H.** The tissue inhibitors of metalloproteinases (TIMPs): an ancient family with structural and functional diversity. *Biochim Biophys Acta* 1803: 55–71, 2010. doi:10.1016/j.bbamcr.2010.01.003.
7. **Cappellari O, Cossu G.** Pericytes in development and pathology of skeletal muscle. *Circ Res* 113: 341–347, 2013. doi:10.1161/CIRCRESAHA.113.300203.
8. **Chaillou T, Jackson JR, England JH, Kirby TJ, Richards-White J, Esser KA, Dupont-Versteegden EE, McCarthy JJ.** Identification of a conserved set of upregulated genes in mouse skeletal muscle hypertrophy and regrowth. *J Appl Physiol (1985)* 118: 86–97, 2015. doi:10.1152/japplphysiol.00351.2014.
9. **Chen CW, Okada M, Proto JD, Gao X, Sekiya N, Beckman SA, Corselli M, Crisan M, Saparov A, Tobita K, Péault B, Huard J.** Human pericytes for ischemic heart repair. *Stem Cells* 31: 305–316, 2013. doi:10.1002/stem.1285.
10. **Chen Y, Lun AT, Smyth GK.** From reads to genes to pathways: differential expression analysis of RNA-Seq experiments using Rsubread and the edgeR quasi-likelihood pipeline. *F1000Res* 5: 1438, 2016. doi:10.12688/f1000research.8987.2.
11. **Crisan M, Corselli M, Chen WC, Péault B.** Perivascular cells for regenerative medicine. *J Cell Mol Med* 16: 2851–2860, 2012. doi:10.1111/j.1582-4934.2012.01617.x.
12. **Crisan M, Yap S, Casteilla L, Chen CW, Corselli M, Park TS, Andriolo G, Sun B, Zheng B, Zhang L, Norotte C, Teng PN, Traas J, Schugar R, Deasy BM, Badylak S, Buhring HJ, Giacobino JP, Lazzari L, Huard J, Péault B.** A perivascular origin for mesenchymal stem cells in multiple human organs. *Cell Stem Cell* 3: 301–313, 2008. doi:10.1016/j.stem.2008.07.003.
13. **Damas F, Phillips SM, Libardi CA, Vechin FC, Lixandrão ME, Jannig PR, Costa LA, Bacurau AV, Snijders T, Parise G, Tricoli V, Roschel H, Ugrinowitsch C.** Resistance training-induced changes in integrated myofibrillar protein synthesis are related to hypertrophy only after attenuation of muscle damage. *J Physiol* 594: 5209–5222, 2016. doi:10.1113/JP272472.
14. **De Lisio M, Farup J, Sukiennik RA, Clevenger N, Nallabelli J, Nelson B, Ryan K, Rahbek SK, de Paoli F, Vissing K, Boppart MD.** The acute response of pericytes to muscle-damaging eccentric contraction and protein supplementation in human skeletal muscle. *J Appl Physiol (1985)* 119: 900–907, 2015. doi:10.1152/japplphysiol.01112.2014.
15. **Dellavalle A, Maroli G, Covarello D, Azzoni E, Innocenzi A, Perani L, Antonini S, Sambasivan R, Brunelli S, Tajbakhsh S, Cossu G.** Pericytes resident in postnatal skeletal muscle differentiate into muscle fibres and generate satellite cells. *Nat Commun* 2: 499, 2011. doi:10.1038/ncomms1508.
16. **Dennis RA, Zhu H, Kortebein PM, Bush HM, Harvey JF, Sullivan DH, Peterson CA.** Muscle expression of genes associated with inflammation, growth, and remodeling is strongly correlated in older adults with resistance training outcomes. *Physiol Genomics* 38: 169–175, 2009. doi:10.1152/physiolgenomics.00056.2009.
17. **DiPasquale DM, Cheng M, Billich W, Huang SA, van Rooijen N, Hornberger TA, Koh TJ.** Urokinase-type plasminogen activator and macrophages are required for skeletal muscle hypertrophy in mice. *Am J Physiol Cell Physiol* 293: C1278–C1285, 2007. doi:10.1152/ajpcell.00201.2007.
18. **Doni A, Musso T, Morone D, Bastone A, Zambelli V, Sironi M, Castagnoli C, Cambieri I, Stravalaci M, Pasqualini F, Laface I, Valentino S, Tartari S, Ponzetta A, Maina V, Barbieri SS, Tremoli E, Catapano AL, Norata GD, Bottazzi B, Garlanda C, Mantovani A.** An acidic microenvironment sets the humoral pattern recognition molecule PTX3 in a tissue repair mode. *J Exp Med* 212: 905–925, 2015. doi:10.1084/jem.20141268.
19. **Egner IM, Bruusgaard JC, Gundersen K.** Satellite cell depletion prevents fiber hypertrophy in skeletal muscle. *Development* 143: 2898–2906, 2016. doi:10.1242/dev.134411.
20. **Fry CS, Kirby TJ, Kosmac K, McCarthy JJ, Peterson CA.** Myogenic progenitor cells control extracellular matrix production by fibroblasts during skeletal muscle hypertrophy. *Cell Stem Cell* 20: 56–69, 2017. doi:10.1016/j.stem.2016.09.010.
21. **Geevarghese A, Herman IM.** Pericyte-endothelial crosstalk: implications and opportunities for advanced cellular therapies. *Transl Res* 163: 296–306, 2014. doi:10.1016/j.trsl.2014.01.011.
22. **Goh Q, Millay DP.** Requirement of myomaker-mediated stem cell fusion for skeletal muscle hypertrophy. *eLife* 6: e20007, 2017. doi:10.7554/eLife.20007.
23. **Guimarães-Camboa N, Cattaneo P, Sun Y, Moore-Morris T, Gu Y, Dalton ND, Rockenstein E, Masliah E, Peterson KL, Stallcup WB, Chen J, Evans SM.** Pericytes of multiple organs do no behave as mesenchymal stem cells in vivo. *Cell Stem Cell* 20: 345–359.e5, 2017. doi:10.1016/j.stem.2016.12.006.
24. **Hume DA, MacDonald KP.** Therapeutic applications of macrophage colony-stimulating factor-1 (CSF-1) and antagonists of CSF-1 receptor (CSF-1R) signaling. *Blood* 119: 1810–1820, 2012. doi:10.1182/blood-2011-09-379214.
25. **Huntsman HD, Zachwieja N, Zou K, Ripchik P, Valero MC, De Lisio M, Boppart MD.** Mesenchymal stem cells contribute to vascular growth in skeletal muscle in response to eccentric exercise. *Am J Physiol Heart Circ Physiol* 304: H72–H81, 2013. doi:10.1152/ajpheart.00541.2012.

26. **Hyldahl RD, Hubal MJ.** Lengthening our perspective: morphological, cellular, and molecular responses to eccentric exercise. *Muscle Nerve* 49: 155–170, 2014. doi:10.1002/mus.24077.
27. **Jung M, Ören B, Mora J, Mertens C, Dziumbla S, Popp R, Weigert A, Grossmann N, Fleming I, Brüne B.** Lipocalin 2 from macrophages stimulated by tumor cell-derived sphingosine 1-phosphate promotes lymphangiogenesis and tumor metastasis. *Sci Signal* 9: ra64, 2016. doi:10.1126/scisignal.aaf3241.
28. **Lau WY, Blazevich AJ, Newton MJ, Wu SS, Nosaka K.** Reduced muscle lengthening during eccentric contractions as a mechanism underpinning the repeated-bout effect. *Am J Physiol Regul Integr Comp Physiol* 308: R879–R886, 2015. doi:10.1152/ajpregu.00338.2014.
29. **Leek JT, Storey JD.** Capturing heterogeneity in gene expression studies by surrogate variable analysis. *PLoS Genet* 3: 1724–1735, 2007. doi:10.1371/journal.pgen.0030161.
30. **Leek JT, Storey JD.** A general framework for multiple testing dependence. *Proc Natl Acad Sci USA* 105: 18718–18723, 2008. doi:10.1073/pnas.0808709105.
31. **Mandel ER, Uchida C, Nwadozi E, Makki A, Haas TL.** Tissue inhibitor of metalloproteinase 1 influences vascular adaptations to chronic alterations in blood flow. *J Cell Physiol* 232: 831–841, 2017. doi:10.1002/jcp.25491.
32. **McCarthy JJ, Mula J, Miyazaki M, Erfani R, Garrison K, Farooqui AB, Srikuea R, Lawson BA, Grimes B, Keller C, Van Zant G, Campbell KS, Esser KA, Dupont-Versteegden EE, Peterson CA.** Effective fiber hypertrophy in satellite cell-depleted skeletal muscle. *Development* 138: 3657–3666, 2011. doi:10.1242/dev.068858.
33. **Mendias CL, Schwartz AJ, Grekin JA, Gumucio JP, Sugg KB.** Changes in muscle fiber contractility and extracellular matrix production during skeletal muscle hypertrophy. *J Appl Physiol (1985)* 122: 571–579, 2017. doi:10.1152/japplphysiol.00719.2016.
34. **Munroe M, Dvoretskiy S, Lopez A, Leong J, Dyle MC, Kong H, Adams CM, Boppart MD.** Pericyte transplantation improves skeletal muscle recovery following hindlimb immobilization. *FASEB J* 33: 7694–7706, 2019. doi:10.1096/fj.201802580R.
35. **Murach KA, White SH, Wen Y, Ho A, Dupont-Versteegden EE, McCarthy JJ, Peterson CA.** Differential requirement for satellite cells during overload-induced muscle hypertrophy in growing versus mature mice. *Skelet Muscle* 7: 14, 2017. doi:10.1186/s13395-017-0132-z.
36. **Murfee WL, Skalak TC, Peirce SM.** Differential arterial/venous expression of NG2 proteoglycan in perivascular cells along microvessels: identifying a venule-specific phenotype. *Microcirculation* 12: 151–160, 2005. doi:10.1080/10739680590904955.
37. **Naito Y, Takagi T, Higashimura Y.** Heme oxygenase-1 and anti-inflammatory M2 macrophages. *Arch Biochem Biophys* 564: 83–88, 2014. doi:10.1016/j.abb.2014.09.005.
38. **Peake JM, Neubauer O, Della Gatta PA, Nosaka K.** Muscle damage and inflammation during recovery from exercise. *J Appl Physiol (1985)* 122: 559–570, 2017. doi:10.1152/japplphysiol.00971.2016.
39. **Péault B, Rudnicki M, Torrente Y, Cossu G, Tremblay JP, Partridge T, Gussoni E, Kunkel LM, Huard J.** Stem and progenitor cells in skeletal muscle development, maintenance, and therapy. *Mol Ther* 15: 867–877, 2007. doi:10.1038/mt.sj.6300145.
40. **Relaix F, Zammit PS.** Satellite cells are essential for skeletal muscle regeneration: the cell on the edge returns centre stage. *Development* 139: 2845–2856, 2012. doi:10.1242/dev.069088.
41. **Robinson MD, Oshlack A.** A scaling normalization method for differential expression analysis of RNA-seq data. *Genome Biol* 11: R25, 2010. doi:10.1186/gb-2010-11-3-r25.
42. **Sacchetti B, Funari A, Remoli C, Giannicola G, Kogler G, Liedtke S, Cossu G, Serafini M, Sampaolesi M, Tagliafico E, Tenedini E, Saggio I, Robey PG, Riminucci M, Bianco P.** No identical "mesenchymal stem cells" at different times and sites: human committed progenitors of distinct origin and differentiation potential are incorporated as adventitial cells in microvessels. *Stem Cell Rep* 6: 897–913, 2016. doi:10.1016/j.stemcr.2016.05.011.
43. **Sambasivan R, Yao R, Kissenpfennig A, Van Wittenberghe L, Paldi A, Gayraud-Morel B, Guenou H, Malissen B, Tajbakhsh S, Galy A.** Pax7-expressing satellite cells are indispensable for adult skeletal muscle regeneration. *Development* 138: 3647–3656, 2011. doi:10.1242/dev.067587.
44. **Sen B, Xie Z, Case N, Ma M, Rubin C, Rubin J.** Mechanical strain inhibits adipogenesis in mesenchymal stem cells by stimulating a durable beta-catenin signal. *Endocrinology* 149: 6065–6075, 2008. doi:10.1210/en.2008-0687.
45. **Shiraki A, Kotooka N, Komoda H, Hirase T, Oyama JI, Node K.** Pentraxin-3 regulates the inflammatory activity of macrophages. *Biochem Biophys Rep* 5: 290–295, 2016. doi:10.1016/j.bbrep.2016.01.009.
46. **Snijders T, Nederveen JP, Joanisse S, Leenders M, Verdijk LB, van Loon LJ, Parise G.** Muscle fibre capillarization is a critical factor in muscle fibre hypertrophy during resistance exercise training in older men. *J Cachexia Sarcopenia Muscle* 8: 267–276, 2017. doi:10.1002/jcsm.12137.
47. **Sugg KB, Korn MA, Sarver DC, Markworth JF, Mendias CL.** Inhibition of platelet-derived growth factor signaling prevents muscle fiber growth during skeletal muscle hypertrophy. *FEBS Lett* 591: 801–809, 2017. doi:10.1002/1873-3468.12571.
48. **Tello-Montoliu A, Patel JV, Lip GY.** Angiogenin: a review of the pathophysiology and potential clinical applications. *J Thromb Haemost* 4: 1864–1874, 2006. doi:10.1111/j.1538-7836.2006.01995.x.
49. **Tidball JG, Dorshkind K, Wehling-Henricks M.** Shared signaling systems in myeloid cell-mediated muscle regeneration. *Development* 141: 1184–1196, 2014. doi:10.1242/dev.098285.
50. **Valero MC, Huntsman HD, Liu J, Zou K, Boppart MD.** Eccentric exercise facilitates mesenchymal stem cell appearance in skeletal muscle. *PLoS One* 7: e29760, 2012. doi:10.1371/journal.pone.0029760.
51. **Wahlberg E.** Angiogenesis and arteriogenesis in limb ischemia. *J Vasc Surg* 38: 198–203, 2003. doi:10.1016/S0741-5214(03)00151-4.
52. **Weis N, Weigert A, von Knethen A, Brüne B.** Heme oxygenase-1 contributes to an alternative macrophage activation profile induced by apoptotic cell supernatants. *Mol Biol Cell* 20: 1280–1288, 2009. doi:10.1091/mbc.e08-10-1005.
53. **Zou K, Huntsman HD, Carmen Valero M, Adams J, Skelton J, De Lisio M, Jensen T, Boppart MD.** Mesenchymal stem cells augment the adaptive response to eccentric exercise. *Med Sci Sports Exerc* 47: 315–325, 2015. doi:10.1249/MSS.0000000000000405.